Beyond Visual Line of Sight UAV Control for Remote Monitoring using Directional Antennas

Songwei Li*, Yixin Gu*, Bishrut Subedi*, Chenyuan He*, Yan Wan*, Atsuko Miyaji† and Teruo Higashino‡
* University of Texas at Arlington, Arlington, TX, USA
† Osaka University, Osaka, Japan
Email: yan.wan@uta.edu

***Abstract*—Many new Unmanned Aerial Vehicle (UAV) applications require beyond visual line of sight (BVLOS) control of UAVs. Examples include UAV-based nondestructive health monitoring of civil infrastructures and remote UAV-assisted emergency response. In this paper, we develop a BVLOS control solution for a remote UAV, using a local UAV relay equipped with automatically aligned directional antennas. The use of UAV relay permits flight control signals to be transmitted even if there exists blockages between the remote UAV and its operator. The use of directional antennas extends the UAV control distance to kilometers with high data throughput. Built upon our previously developed aerial communication system using directional antennas (ACDA), we first upgrade the hardware and software to improve the throughput and endurance. We then design and implement a BVLOS control solution which includes a two-way relay communication. In one direction, low-resolution video views from the remote UAV are transmitted through the local UAV relay to help a UAV operator navigate the remote UAV. In the other direction, UAV control signals are relayed through the local UAV and transmitted to the remote UAV for BVLOS operations. The system is verified using simulation studies and field tests.**

***Index Terms*—Unmanned aerial vehicles, Beyond Visual Line of Sight, Directional Antennas, Robot Operation System**

I. Introduction

Unmanned Aerial Vehicles (UAVs) have found broad commercial use in civilian applications. For instance, UAV-assisted nondestructive health monitoring has been used to monitor bridge infrastructures to avoid catastrophic accidents [1]–[4]. Traditional infrastructure inspections are often performed through a manual visual-based procedure, which are expensive, time-consuming, and even unsafe for some structural parts, e.g., the sides and underneath parts of bridges. Paper [1] studied the feasibility of using UAVs for fatigue crack detection in bridges and demonstrated the field performance using three different types of UAVs. In [2], the authors analyzed different UAV types based on weight, flight type, payload and flight time, and selected a rotary-wing typed drone for crack detection of bridges. Paper [3] used an on-board high definition (HD) camera to collect images of bridges and stored the images in a storage card for further processing and crack detection. Paper [4] used an UAV for concrete crack identification. The UAV transmitted images, distance information and control signals with a human operator in real time through a WiFi module. Similarly, UAV-assisted emergency response has found its significant value in reducing response time and better allocating resources [5]. Paper [5] developed a 3D reconstruction method from UAV images to identify collapsed buildings after earthquakes.

In all existing UAV applications, UAVs are controlled within the visual line of sight. This restriction limits the flexibility and applicability of UAVs. Many UAV applications require the beyond visual line of sight (BVLOS) control. For instance, in emergency response, UAV operators often cannot get close to emergency zones, due to broken roads, debris, or remaining dangers in the zones [6]. The standard communication range, such as Wi-Fi, is not sufficiently long for UAV control. Similarly, in nondestructive health monitoring, an operator may not always be able to keep the UAV within visual sight due to various structural constraints [7]. Blockages should not limit UAV operations.

To address the aforementioned issues, we here aim to develop a BVLOS control solution for UAVs, which extends the operation range to kilometers, and is not limited by blockages between an operator and UAV. Designing BVLOS UAV control is challenging, considering the difficulties such as UAV situation awareness and wireless communication robustness. The research on BVLOS control is limited [8]. Paper [8] describes a transportation system for UAV BVLOS applications based on Long-Term Evolution (LTE). The solution requires LTE support and hence can be expensive. There is a need to implement UAV BVLOS control using a communication system that is cost-effective and can be quickly deployed without ground infrastructure support.

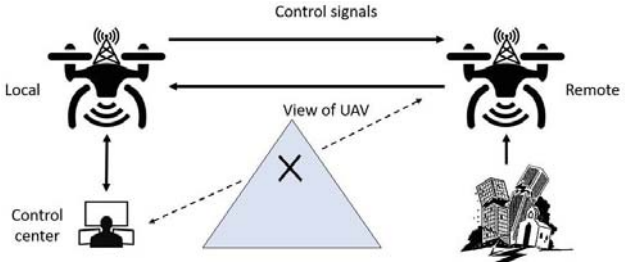

Fig. 1: Illustration of the teleoperation of the remote UAV based on the ACDA system

The BVLOS UAV control solution we design in this paper is shown in Fig 1. The solution is based on a long-

978-1-7281-0960-2/19/$31.00 ©2019 IEEE

distance and broadband UAV communication system concept we developed previously, called aerial communication using directional antennas (ACDA) [9]–[16]. In [13], we designed and implemented the complete ACDA system, which is composed of two UAV platforms (one for local side, and one for remote side), on-board autopilot, communication component, and autonomous antenna heading alignment. The local UAV platform serves as a network relay and the remote UAV platform is used for monitoring. The two UAVs are dispatched to the air to establish communication, and then the local UAV communicates with the local ground device through an UAV-ground communication channel. The ACDA system does not rely on ground infrastructure support, and hence can be applied to scenarios where fixed communications infrastructures are not available. With the use of directional antennas and an automatic alignment algorithm, the ACDA system features long-range communication and high throughput. In [15], we improved the ACDA system with a unified communication and control channel, an integrated design and implementation of communication, control and computing components and a user-friendly interface. Moreover, we designed a reinforcement learning (RL)-based directional antenna control algorithm that maximizes communication performance in unknown communication environments.

The aforementioned works do not yet realize BVLOS UAV control for the following reasons. First, in the ACDA system, each UAV is controlled locally by a UAV operator. UAV control is within line of sight. In this paper, we transmit the remote UAV's control signal through the ACDA system, to enable BVLOS operations. Second, according to our experimental studies, the ACDA system has some performance limitations in terms of interference and endurance. In this paper, we redesign the ACDA system to conquer these performance limitations. Our contributions in this paper are summarized as follows.

The first contribution is the design of BVLOS UAV control, using the ACDA system with a local UAV relay. The use of UAV relay permits flight control signals to be transmitted even if there exists blockages between the UAV and its operator. The use of directional antennas extends the UAV control distance to kilometers with high data throughput. The BVLOS control solution includes a two-way relay communication. In one direction, low-resolution videos from the remote UAV is transmitted through the local UAV relay to help UAV operator navigate the remote UAV. The low resolution videos are for the navigation purpose. They provide situation awareness to UAV operators and also allow operator to locate targets of interest, such as structural defects in health monitoring and victims in emergency response. In the other direction, UAV control signals are relayed through the local UAV and transmitted to the remote UAV for BVLOS navigation. High-resolution videos from the remote UAV can be stored in a storage card for further processing. We design a remote control solution to operate the remote UAV using a keyboard at the local side of the ACDA system.

The second contribution lies in the ACDA redesign to enhance its performance. In particular, the microprocessor is changed from Beaglebone Black to NVIDIA Jetson TX2 Module (TX2) to improve the computing capability. In addition, the UAV platform is changed from DJI Matrice 100 to Tarot 650 to remove the interference between the UAV platform (and in particular Carbon fiber propellers) and the communication system. The flight controller is changed correspondingly from DJI N1 to the open source flight controller Pixhawk. The redesign also includes the rotational structure of directional antennas to improve its endurance with 360 degree rotation capability. In addition, a new rechargeable battery is designed to expand the working hours of the ACDA system. Finally, the propellers, motors, and the battery for UAV are reconfigured to enable 25 minutes of flight time with the desired payload.

The rest of this paper is organized as follows. In Section II, we describe the upgraded ACDA system design in terms of both hardware and software design. Section III describes the BVLOS UAV control using a keyboard through the ACDA relay. The section also includes the verification studies using simulation studies and field tests. Section IV concludes this paper.

II. The ACDA system Design

In this section, we first introduce the ACDA system. Then we describe the design of the upgraded ACDA system in details.

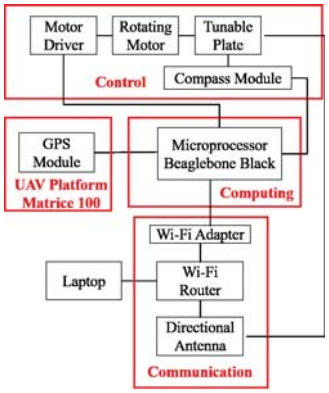

(a) The previous ACDA system

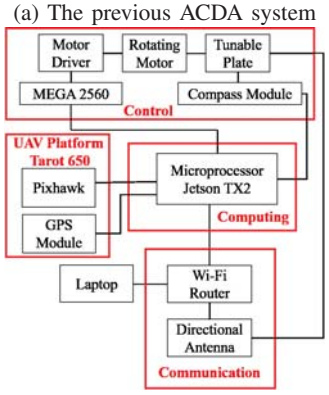

(b) The new ACDA system

Fig. 2: Components comparison between the previous ACDA and the new ACDA system

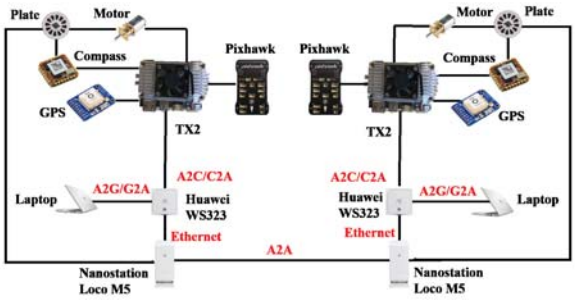

Fig. 3: Illustration of the connections among different components in the ACDA system

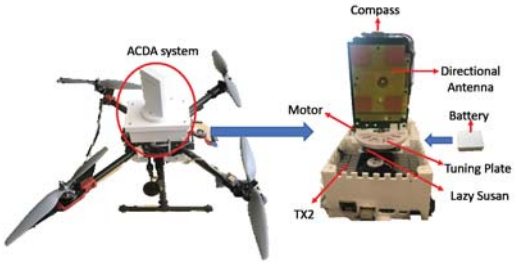

Fig. 4: Tarot 650 and the ACDA system

A. Overview of The ACDA System

In [15], we designed and implemented an ACDA system. The ACDA system is composed of a pair of subsystems on both the local and remote sides. The subsystem on each side is composed of four parts: UAV platform, control component, computing component, and communication component as shown in Fig 2 (a). The connections among different components is shown in Fig 3. The communication component is critical for the ACDA system. It includes Wi-Fi adapter, Wi-Fi router and directional antenna. The types of links include: Air to Ground (A2G)/Ground to Air (G2A), Air to Air (A2A), and Air to Computing module (A2C)/Computing module to Air (C2A) links. The control component rotates the directional antennas automatically using an alignment algorithm so that the system can achieve its best communication capacity. The computing component is responsible for collecting data, processing the computing and learning tasks, and exporting motor control signal to the control component. With an user-friendly interface installed on the local laptop, the ACDA system configuration and system information including the locations of UAVs, distance, communication quality, antenna alignment performance and real-time videos can be displayed in real time.

To improve system performance for BVLOS operation, we upgrade the ACDA system (see Fig 2 (b)). To improve UAV stability, remove interference and enhance communication performance, we changed the UAV platform from DJI Matrice 100 to Tarot 650 with Pixhawk. To improve the computing capability, we use TX2 as the computing component instead of the Beaglebone Black. To achieve better control performance, we adopt a lazy susan bearing component and an Atmega2560 chip for the control component. In addition, a new battery system is assembled to expand the working time of the ACDA system. In the following subsections, we will discuss the improvements in detail.

B. The Upgraded ACDA System Design

1) The UAV Platform: Considering the performance metrics of UAVs such as payload, flight time, expandability, stability, and operability, Matrice 100 [15] and Tarot 650 with Pixhawk [13] (see Fig 4) are two good options. However, the flight control signal operating at $2.4GHz$ and carbon fiber propellers of Matrice 100 can potentially interfere with the ACDA's WiFi router, which also operates at $2.4GHz$. This interference can cut in half of the throughput of the communication capacity. To avoid the interference, we choose Tarot 650 with Pixhawk and plastic propellers ($13inch$) as the UAV platform for the upgraded ACDA system. The flight control signal link of Pixhawk operates at $72MHz$, which does not overlap with the Wi-Fi router so that there is no interference between them. By using plastic propellers, the interference caused by carbon fiber propellers is removed. To extend flight time, we adopt a LiPo battery of $6S$ $10000mAh$ for Tarot 650. In addition, the Pixhawk's TELEM2 (a serial port) is connected with a USB port of TX2 for communication between these two devices.

2) The Communication System: Compared with Beaglebone Black which has no WiFi module, the TX2 has a built-in WiFi unit, hence no external WiFi adapter is needed. The ACDA system has A2G/G2A, A2A, A2C/C2A communication links as shown in Fig 3. Two directional antennas form the A2A link, with an A2G/G2A link on each side provided by a WiFi router. The WiFi router also provides an A2C/C2A link by connecting with the built-in WiFi unit in TX2. Using these three types of wireless communication links, two TX2s on the local side and the remote side collect data from sensors and Pixhawks, and publish these data to the ACDA system using robot operation system (ROS).

3) The Computing Component: The computing component is responsible for all the computing tasks in the ACDA system. In particular, the component is responsible for obtaining data from sensors and Pixhawk, publishing obtained data to ROS, calculating the desired heading of antennas and sending motor's rotation direction and speed to the control component of the ACDA system. In the upgraded ACDA system, TX2 serves as the computing component instead of Beaglebone Black as TX2 has a better computing capability. The TX2's CPU includes a dual-core NVIDIA Denver2 ($2GHz$) and a quad-core ARM Cortex-A57 ($2GHz$). Its GPU is 256-core Pascal. Its CSI2 supports $2.5Gbps/Lane$. Meanwhile, it has $8GB$ $128bit$ LPDDR4 memory and $32GB$ eMMC onboard flash storage. Because the original NVIDIA carrier board of TX2 is too large and heavy to be used for UAV, we design a space-efficient and lightweight carrier board for TX2 with size $88mm \times 65mm$ (87 percent surface shrunk compared to the original carrier board) and weight $53g$ (see Fig 5).

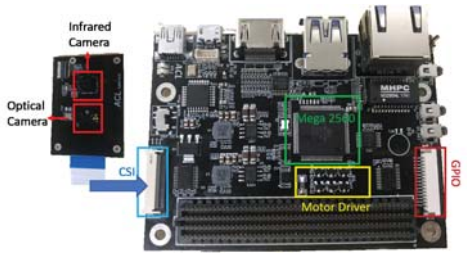

Fig. 5: TX2 customized carried board

4) The Antenna Heading Control Component: The control component drives the geared motors to automatically align the two directional antennas. The control component is consist of an Atmega2560 chip, a H-bridge motor driver, a geared DC motor, a magnetometer and a rotatable plate with a lazy susan turntable (see Fig 4). The Atmega2560 reads the UAV location from the local GPS module and RSSI data from the directional antennas and then sends data to the local TX2. Once TX2 finishes its computing, Atmega2560 receives motor control signals from TX2 and outputs stable PWM signals to the motor driver to drive the motor for antenna control. The Atmega2560 and motor driver are integrated on the compact TX2 carrier board to save space and reduce wires (see Fig 5). In addition, Atmage2560 provides various connection port with TX2, such as I2C, UART, and SPI ports. Atmega2560 and TX2 work together to complete massive computing tasks and output stable PWM signals. For the rotational structure upgrade, we select a lazy susan turntable to connect the rotational parts with non-rotational parts of the system and use a slip ring to connect TX2 with the directional antenna and a built-in compass. Compared with the previous rotational design in [15], this new design guarantees the coaxiality of the tuning plate to avoid shaking. The design has a more stable and smoother antenna rotation.

5) Autonomous Antenna Alignment: Because of the mobility of UAVs, it is necessary to automatically align two antennas to maintain robust communication and achieve the best communication capacity. This task is achieved by an antenna heading control algorithm. Antenna heading control aims to autonomously diminish the difference between the desired and the currently measured headings. The desired heading is calculated from local and remote GPS locations of both UAVs for antenna alignment. The current heading is a direct output of compass reading. The difference is sent to the heading control algorithm [13], which is a Linear Quadratic Gaussian (LQG) controller consisting of a Kalman filter and a linear quadratic regulator (LQR). The Kalman filter is used to estimate the system states $\hat{x}$. The linear quadratic regulator is a state feedback controller. The LQG is used to minimize the quadratic GPS-based tracking error. The LQG controller can be described as $p^* = -K_c\hat{x}$, where p^* is the optimal control input and K_c is the gain matrix of optimal controller sent to the control part to rotate the directional antenna assembly.

6) The Battery Design: The space and payload of the UAV platform restrict the size and weight of the components installed on it. Therefore, a small size, lightweight and high capacity battery is desired for the ACDA system. We could not find a battery in the market with the shape and size suitable for the ACDA system. As such, we design a new rechargeable battery using three Panasonic Li-ion MH12210 and a charge protection circuit board. The output voltage is $12.6V$ and the total capacity is $3250mAH$. The battery can support the ACDA system to work for up to 2 hours, which greatly enhances the durability of the system.

7) Information Flow in ROS: ROS is used to transmit messages between multiple devices in the ACDA system (see Fig 6). TX2 communicates with Atmega2560 using the Rosserial package and with Pixhawk using the MAVROS package. TX2 directly reads the directional antenna heading from a compass module. TX2 subscribes GPS and RSSI ROS topics from Atmega2560 and publishes motor PMW control signals to Atmega2560. In addition, one optical camera (OmniVision OV5693) and one infrared camera (FLIR LEPTON 3) are connected to the remote TX2 via a camera serial interface (CSI). The remote TX2 first launches a ROS video node to obtain a high resolution (up to 2592×1944) image from OV5693. Then it saves the high resolution image in a storage card on the remote TX2. Meanwhile, it converts the high resolution image to a low resolution image (640×480), which is subscribed and displayed through the interface on the local laptop. The low resolution images are used for BVLOS UAV navigation control. For BVLOS UAV control, MAVROS must be executed on the remote TX2 to convert MAVLink messages of Pixhawk to ROS messages. In addition, Pixhawk also subscribes control signals from the remote TX2. The remote TX2 collect videos from an optical camera and an infrared camera and convert videos to ROS image topics. All ROS topics are published in the ROS network. The local laptop subscribes all the messages and displays them on the user-friendly interface which has been introduced in [15]. The local laptop also publishes the control ROS topic to the remote UAV.

III. BVLOS UAV Control

To realize BVLOS UAV control, control signals for the remote side UAV needs to be transmitted through ACDA to the local side. In this section, we develop a BVLOS solution to control the remote UAV from the local side using a keyboard.

A. System Design and Implementation

1) Pixhawk Setup: To enable communication between TX2 and Pixhawk, MAVLink, which is a message protocol, needs to be enabled on a configurable serial port of Pixhawk. TELEM 2 (serial port) is selected to link with a USB port of TX2. The default setting of TELEM 2 port is disabled in Pixhawk's open source flight control software PX4 (V1.9.0). Therefore, we enable the TELEM 2 port using PX4 groundstation QGound-Control (QGC), which provides full flight control and can modify all configurable parameters in PX4. After appropriately

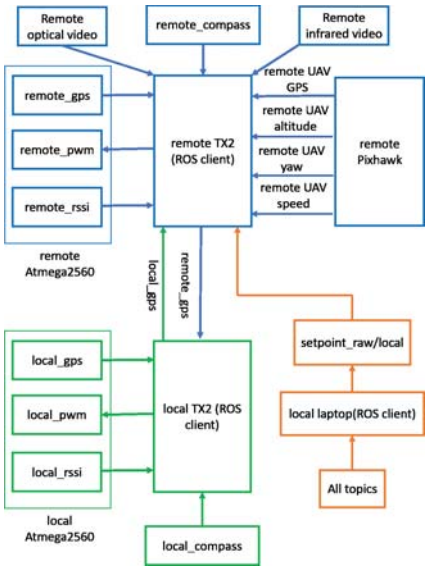

Fig. 6: ROS architecture and topics in the ACDA system.

setting up the serial port configuration, its mode and baud rate, MAVLink is available on the TELEM 2 port.

2) TX2 Setup: In the second step, we need to convert MAVLink messages to ROS messages so that the local laptop can read the messages and completely control the remote UAV. By utilizing ROS, we do not need to build a customized communication link between the local laptop and the remote Pixhawk. We use the MAVROS ROS package to build a bridge between MAVLink messages and ROS topics. MAVROS publishes messages, such as IMU state, local position in the North-East-Down (NED) coordinate, global position information, and system status, to the ACDA system. MAVROS subscribes ROS topics to control UAVs, including the local position, velocity, acceleration, attitude, angular rate and thrust of a UAV in the local coordinate. In addition, MAVROS includes some services to control UAV mobility, such as waypoint service to set up waypoints, param service to access the parameters of PX4, and command services to send arm, takeoff, land commands to Pixhawk and check UAV status.

After MAVROS is installed on TX2, MAVLink messages can be converted to ROS topics by executing ROS PX4 node through a command in the terminal window of TX2. By setting up the linked port and baud rate, Pixhawk and TX2 are successfully connected, and hence Pixhawk and the ACDA system. The communication from MAVLink messages to ROS topics is shown in Fig 7 (a).

3) Teleoperation: In MAVLink protocol, there are two commands for off-board control of PX4 flight, set position command and set attitude command. Likewise, we have two ROS topics corresponding to these two commands in MAVROS. In this paper, we only use set position command for the BVLOS control of remote UAV. The message of the set position command includes flight control parameters coordinate (NED or body coordinate), position, velocity, acceleration, yaw and yaw rate. We control the UAV with the velocity (VX, VY, VZ) and yaw in the body coordinate of the UAV. We select the body coordinate to do off-board control, and assign ignore flag to position, acceleration and yaw parameters. As shown in Fig 7 (b), the body coordinate in MAVROS is Right_Forward_Up (RFU). The body coordinate in MAVLink is Forward_Right_Up (FRU). Therefore, there is a coordinate transformation between MAVROS and MAVLink.

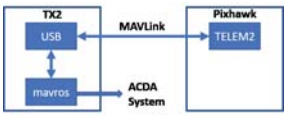

(a) The communication from MAVLink message to ROS Topics

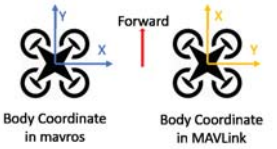

(b) The Body Coordinate of the UAV in MAVROS and MAVLink

Fig. 7: BVLOS UAV control message flow and body coordinate of the UAV

We use eight keys on a standard keyboard to control UAV movements. In particular, move forward, backward, left, right, upward, downward, rotate clockwise, rotate counterclockwise, and hover in the air. In addition, if the time between two offboard commands exceeds 0.5 second, the flight mode of the PX4 goes out of the offboard mode and restores the last mode of the Pixhawk. As such, the frequency of sending offboard commands must be larger than $2Hz$.

B. Simulation Studies

1) Simulation Environment: Before realizing the offboard control on a real UAV, it is necessary to simulate and debug it through software. PX4 provides such capability. According to [17], PX4 supports the Hardware In the Loop (HITL) simulation with Gazebo simulator [18], which is a powerful simulation tool that is compatible with ROS. In order to simulate PX4 in Gazebo, PX4 firmware must be installed in the ROS work space on a laptop with the Ubuntu operation system. PX4 Firmware in the Gazebo environment allows the simulation of multiple UAVs. In addition, they can also simulate the data from all sensors, including IMU, GPS, camera and barometer modules. They can even simulate the wind environment for the simulated UAVs and create noise to corrupt GPS signals. In this case, we set up an ideal simulation environment without wind and noise.

2) BVLOS UAV Control Simulation with Gazebo: First, create a Quadcopter in the Gazebo simulator. Second, connect the simulated Quadcopter with ROS by launching a MAVROS package at a specified port through User Datagram Protocol (UDP) protocol. Becuase we simulate our offboard program on one laptop, the IP address of the laptop is the locallhost. An offboard API transmits messages with PX4 for ROS initial connection. Third, open QGC to monitor the Quadcopter's movement and status. Finally, execute BVLOS UAV control. In this simulation, we make the Quadcopter move a 'Z' trajectory. The simulation result is shown in the Fig 8.

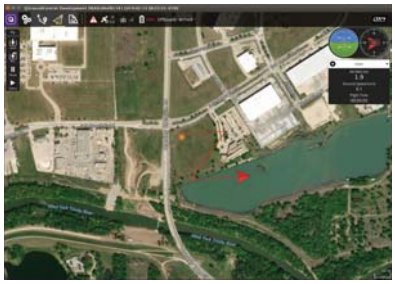

Fig. 8: BVLOS UAV Control in Gazebo using ROS

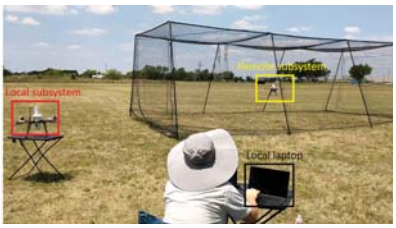

Fig. 9: Test of the teleoperation in the ACDA system

C. Field Tests

To test performance of the ACDA system, we let the local and remote UAV fly at the same altitude, and then we measure the end-to-end communication performance between the local laptop and remote laptop by Iperf. The throughput of the ACDA system is measured with different distances as

Distance	1000 m	2000 m	4000 m
Throughput	45 Mbps	40 Mbps	20 Mbps

We also test the BVLOS UAV control. As shown in Fig 9, the remote UAV is placed in the net to comply with FAA regulations. The wind speed is less than $10mph$. On the local side, the laptop displays the interface to monitor the status of the ACDA system and live videos transmitted from the remote side. Another local laptop runs the BVLOS control. Experimental results show that we can successfully control the remote UAV using keyboard through the local UAV relay in the ACDA system.

IV. Conclusions and Future Works

ACDA is a long-distance and broad-band UAV-to-UAV communication system. In this paper, we redesign the ACDA system in terms of hardware and software to improve the throughput and endurance for BVLOS UAV control. In particular, we change the UAV platform and propellers to reduce interference, upgrade the computing component of ACDA with TX2 to enhance computing capability, design a battery solution to extend the ACDA's working time, and improve the rotation structure of the directional antenna to enhance the mechanical endurance of the turning plate. To realize BVLOS operation, we transmit the remote UAV control to the local side by connecting Pixhawk to the ACDA system via MAVROS. The performance of the BVLOS UAV control system is verified using simulation and a set of field test studies. The BVLOS UAV control system can be applied to many applications, such as health monitoring, surveillance and reconnaissance.

Acknowledgment

This work is partially supported by NSF Grants 1714519 and 1730675.

References

[1] S. Dorafshan, R. J. Thomas, and M. Maguire, "Fatigue crack detection using unmanned aerial systems in fracture critical inspection of steel bridges," *Journal of bridge engineering*, vol. 23, no. 10, p. 04018078, 2018.

[2] J.-W. Kim, S.-B. Kim, J.-C. Park, and J.-W. Nam, "Development of crack detection system with unmanned aerial vehicles and digital image processing," in *Proceedings of 2015 World Congress on Advances in Structural Engineering and Mechanics (ASEM15)*, Incheon, Korea, August 2015.

[3] H. Yu, W. Yang, H. Zhang, and W. He, "A uav-based crack inspection system for concrete bridge monitoring," in *Proceedings of 2017 IEEE International Geoscience and Remote Sensing Symposium (IGARSS)*, Fort Worth, TX, July 2017.

[4] H. Kim, J. Lee, E. Ahn, S. Cho, M. Shin, and S.-H. Sim, "Concrete crack identification using a uav incorporating hybrid image processing," *Sensors*, vol. 17, no. 9, p. 2052, 2017.

[5] K. Ogura, Y. Yamada, S. Kajita, H. Yamaguchi, T. Higashino, and M. Takai, "Ground object recognition from aerial image-based 3d point cloud," in *Proceddings of 2018 Eleventh International Conference on Mobile Computing and Ubiquitous Network (ICMU)*, Oct 2018, pp. 1–8.

[6] J. Han, Y. Xu, L. Di, and Y. Chen, "Low-cost multi-uav technologies for contour mapping of nuclear radiation field," *Journal of Intelligent Robotic Systems*, vol. 70, no. 1-4, pp. 401–410, 2013.

[7] M. Asnafi and S. Dastgheibifard, "A review on potential applications of unmanned aerial vehicle for construction industry," *Sustainable Structures and Materials, An International Journal*, vol. 1, no. 2, pp. 44–53, 2018.

[8] H. Menouar, I. Guvenc, K. Akkaya, A. S. Uluagac, A. Kadri, and A. Tuncer, "Uav-enabled intelligent transportation systems for the smart city: Applications and challenges," *IEEE Communications Magazine*, vol. 55, no. 3, pp. 22–28, March 2017.

[9] Y. Gu, M. Zhou, S. Fu, and Y. Wan, "Airborne wifi networks through directional antennae: An experimental study," in *Proceedings of 2015 IEEE Wireless Communications and Networking Conference (WCNC)*, New Orleans, LA, March 2015.

[10] Y. Wan, S. Fu, J. Zander, and P. J. Mosterman, "Transforming on-demand communications with drones: The needs, analyses, and solutions," *Homeland Security Today Magazine*, pp. 32–35, 2015.

[11] S. Fu and Y. Wan, "Communicating in remote areas or disaster situations using unmanned aerial vehicles," *HDIAC Journal*, vol. 2, no. 4, pp. 4–8, 2016.

[12] J. Xie, F. AI-Emrani, Y. Gu, Y. Wan, and S. Fu, "Uav-carried long-distance wi-fi communication infrastructure," in *Proceedings of AIAA Infotech@ Aerospace*, San Diego, California, January 2016.

[13] J. Chen, J. Xie, Y. Gu, S. Li, S. Fu, Y. Wan, and K. Lu, "Long-range and broadband aerial communication using directional antennas (acda): Design and implementation," *IEEE Transactions on Vehicular Technology*, vol. 66, no. 12, pp. 10 793–10 805, Dec 2017.

[14] J. Yan, Y. Wan, S. Fu, J. Xie, S. Li, and K. Lu, "Received signal strength indicator-based decentralised control for robust long-range aerial networking using directional antennas," *IET Control Theory & Applications*, vol. 11, pp. 1838–1847, 2017.

[15] S. Li, C. He, M. Liu, Y. Wan, Y. Gu, J. Xie, S. Fu, and K. Lu, "The design and implementation of aerial communication using directional antennas: Learning control in unknown communication environments," *IET Control Theory Applications*, April 2019.

[16] K. Lu, J. Xie, Y. Wan, and S. Fu, "Toward uav-based airborne computing," *IEEE Wireless Communications*, 2019.

[17] PX4, "Px4 user guide." [Online]. Available: https://docs.px4.io/en/

[18] Gazebo, "Gazebo simulator," *gazebosim.org*. [Online]. Available: http://gazebosim.org/